

1
2
3
4
5
6
7
8
9
10
11
12
13
14
15
16
17
18
19
20
21

Density fractionation and ^{13}C reveal changes in soil carbon following woody
encroachment in a desert ecosystem

Heather L. Throop^{1*}, Kate Lajtha², Marc Kramer³

¹Biology Department, New Mexico State University, Las Cruces, NM 88003, USA

²Crop and Soil Science Department, Oregon State University, Corvallis, OR 97331,
USA

³Department of Geology, Portland State University, Portland, OR 97207, USA

*corresponding author, throop@nmsu.edu, 575-646-5970 (voice), 575-646-5665 (fax)

22 **Abstract**

23 Woody encroachment has dramatically changed land cover patterns in arid and semiarid
24 systems (drylands) worldwide over the past 150 years. This change is known to influence bulk
25 soil carbon (C) pools, but the implications for dynamics and stability of these pools are not well
26 understood. Working in a Chihuahuan Desert C₄ grassland encroached by C₃ creosote bush
27 (*Larrea tridentata*), we used two density fractionation techniques (2 and 7 pool density
28 fractionations) and isotopic analysis to quantify changes in C pools and dynamics among
29 vegetation microsites typical of an encroachment scenario (remnant intact grassland, shrub
30 subcanopies, and in shrub intercanopy spaces within a shrub-encroached area). The C
31 concentration of bulk soils varied with microsite, with almost twice the C in shrub subcanopies
32 as in intercanopy spaces or remnant grasslands. Estimated SOC accumulation rates from
33 *Larrea* encroachment (4.79 g C m⁻² y⁻¹ under canopies and 1.75 g C m⁻² y⁻¹ when intercanopy
34 losses were taken into account) were lower than reported for higher productivity *Prosopis*
35 systems, but still represent a potentially large regional C sink. The composition of soil C varied
36 among microsites, with the shrub subcanopy C composed of proportionally more light fraction C
37 (<1.85 g cm⁻³) and C that was soluble in sodium polytungstate. Grassland soils contained very
38 little carbonate C compared to shrub subcanopies or shrub intercanopy spaces. Stable isotope
39 analyses indicate that inputs from C₃ shrubs were incorporated into all density fractions, even in
40 heavy fractions in which shrub inputs did not change overall C concentration. The seven
41 density fractionation yielded unexpected δ¹³C patterns, where the two heaviest fractions were
42 strongly depleted in ¹³C, indicating strong fractionation following organic matter inputs. These
43 results suggest that the utility of isotope mixing models for determining input sources may be
44 limited in systems with similar fractionation patterns. We propose a five pool model for dryland
45 soil C that includes a relatively dynamic light fraction, aggregate and heavy fractions that are
46 stable in size but that reflect dynamic inputs and outputs, a potentially large and seasonally

47 dynamic pool of soluble C, and a large pool of carbonate C. Combined, these results suggest
48 that dryland soil C pools may be more dynamic than previously recognized.

49

50 **Keywords:** *Larrea*, *Bouteloua*, soil organic matter, dryland, carbonates, soil carbon

51 stabilization, woody encroachment

52

53 **Introduction**

54 Soil organic carbon (SOC) is a major component of the global carbon (C) cycle, accounting for
55 more C than the terrestrial biomass and atmospheric pools combined (Amundson 2001). The
56 annual CO₂ flux from soils to the atmosphere is >10 times that from fossil fuel combustion
57 (Schlesinger 1997), so small changes in SOC pools have the potential to greatly influence the
58 atmospheric CO₂ concentration and subsequently affect Earth's climate. Arid and semi-arid
59 ecosystems (hereafter 'drylands') cover 40% of the terrestrial land surface and account for 30-
60 35% of terrestrial net primary productivity (Bailey 1996; Field et al. 1998), making them a major
61 component of the global C cycle. While SOC *concentrations* in dryland soils are typically low,
62 extensive land cover change and human disturbances in these areas alter the *fluxes* between
63 atmospheric and SOC pools. Integrated over the large geographical extent of drylands, these
64 flux changes may represent a significant source or sink of atmospheric C (Lal 2004). Woody
65 encroachment, an increase in woody plant cover in formerly grass-dominated ecosystems, may
66 currently be dramatically altering the sink strength of dryland soils. Modeling and field-based
67 inventories suggest that geographically extensive woody proliferation in drylands accounts for a
68 potentially large, although highly uncertain, portion of the North American C sink. For example,
69 Pacala *et al.* (2001) estimate that woody encroachment in drylands accounts for 18-40% of the
70 C sink in the continental United States. Understanding the current and future dynamics of this
71 terrestrial sink requires understanding both how vegetation change affects SOC pools and
72 controls over the stability of these pools.

73
74 Woody encroachment has fundamentally changed many of the world's drylands over the past
75 150 years (Archer 1994). While the causes of this land cover change are subject to
76 considerable debate, changes in land management practices (particularly increased grazing
77 pressure and decreased fire frequency) appear to be major factors (Archer et al. 2001). Climate
78 change, exotic species, N deposition, and atmospheric CO₂ enrichment may also play a role

79 (Archer 1994; Archer 1995; Van Auken 2000). Several recent syntheses suggest that
80 aboveground C typically increases with woody encroachment. The magnitude of this change is
81 positively related to mean annual precipitation, with net losses in aboveground C possible in
82 very dry sites or with increased fire frequency (Barger et al. 2011; Eldridge et al. 2011; Knapp et
83 al. 2008). A synthetic understanding of belowground C responses to woody encroachment has
84 proven more elusive; the magnitude, and even direction (positive, negative, or neutral) of
85 belowground C change in response to woody encroachment remains difficult to generalize
86 (reviewed in Wessman et al. 2004; Barger et al. 2011). The prevailing dogma for dryland woody
87 encroachment has been that woody plants create “islands of fertility” where SOC and soil
88 nutrients accumulate due to changes in litter input quality and quantity (e.g., Garcia-Moya and
89 McKell 1970; Schlesinger et al. 1990). Woody plants may also promote nutrient accumulation in
90 subcanopy zones by translocating nutrients from intercanopy areas, enhancing deposition from
91 aeolian, fluvial or animal transport processes (Belsky et al. 1989; Okin and Gillette 2001; Weltz
92 et al. 1998; Lajtha and Schlesinger 1986) or slowing organic matter losses through depressed
93 subcanopy decomposition (Throop and Archer 2007). The distribution of inputs may also shift,
94 with greater root biomass in shrub subcanopy patches than intact grasslands (Hibbard et al.
95 2001), and a deeper distribution of woody roots than herbaceous roots (Jackson et al. 1996).
96 Improving generalizations about the consequence of woody encroachment to SOC pools and
97 dynamics is crucial to reducing uncertainty about ecosystem C storage responses to woody
98 encroachment.

99

100 One challenge to understanding and generalizing woody encroachment impacts on SOC is that
101 the majority of SOC analyses in drylands to date has focused on *bulk* SOC pools. SOC exists in
102 various states of chemical, physical, or biological stabilization. As such, SOC consists of pools
103 that vary in turnover rates, from highly labile pools (e.g., surface detritus that often persists for
104 <1 year) to those that persist for decades to millennia (e.g., C in highly stabilized organo-mineral

105 complexes; Trumbore 2000). The controls over the formation and destabilization of organo-
106 mineral complexes are still not well understood, particularly in the context of soil disturbance or
107 changing vegetation or climate (e.g., Diochon and Kellman 2009; Kane et al. 2005). Data on
108 bulk (whole soil) SOC provide a short-term snapshot of C pools, but provide limited insight into
109 long-term C dynamics (Trumbore 2000; Trumbore et al. 1995). In drylands, SOC may
110 accumulate for many decades to centuries following initial woody encroachment (Liao et al.
111 2006b; Throop and Archer 2008; Wheeler et al. 2007) and SOC may persist following woody
112 plant removal for > 4 decades (McClaran et al. 2008). Understanding controls over SOC
113 stability is crucial for understanding under what conditions SOC will persist, and whether
114 changes in bulk pools are likely to translate into long-term storage. Furthermore, understanding
115 controls over SOC stabilization is crucial for developing and parameterizing models that can
116 accurately predict SOC dynamics under future climate, vegetation, and land management
117 scenarios (e.g., Hatton et al. 2012; Parton et al. 1993; Parton et al. 1988).

118

119 A variety of physical, chemical, and biological fractionation techniques have been used to
120 separate out meaningful fractions of SOC that differ in relative stability (Christensen 2002; Crow
121 et al. 2007; McLauchlan and Hobbie 2004). While no single universally accepted method exists,
122 separation of soils into two or more density fractions via floatation provides functionally-relevant
123 information on both associations between organic material and mineral particles and their
124 stability (Baisden et al. 2002; Crow et al. 2007; Sollins et al. 2006). The density of soil particles
125 varies as a function of organic matter concentration, mineral particle density, and particle
126 porosity (Sollins et al. 2009). Previous work in mesic systems suggests that sequential density
127 fractionation (SDF) divides soil into fractions that differ in both mineralogy and organic matter
128 composition (Sollins et al. 2009; Sollins et al. 2006). Organic matter concentration typically
129 decreases with increasing particle density, and C:N ratios, $\delta^{13}\text{C}$, and other biochemical indices
130 suggest that organic matter associated with denser particles has undergone greater microbial

131 processing than that associated with less dense particles. Furthermore, radiocarbon dating
132 indicates that C associated with denser particles typically has a greater mean residence time
133 (Sollins et al. 2009). To date, SDF has been performed in relatively mesic systems, and it is
134 unclear whether the patterns observed in those systems would hold under the different climate
135 and soil composition of drylands. However, SDF procedures are expensive and time intensive,
136 and thus are typically performed on unreplicated soil samples (e.g., Sollins et al. 2009), limiting
137 their relevance for understanding ecological patterns that differ in time and space. However,
138 SDF procedures could be combined with other less time intensive and expensive
139 measurements (e.g., two pool density fractionation or incubation techniques), thus allowing
140 inferences from SDF to be extended through time or space.

141

142 We coupled density fraction techniques and stable isotope analyses to explore changes in SOC
143 composition and input sources following woody encroachment by creosote bush, *Larrea*
144 *tridentata*, in a former grassland in the northern Chihuahuan Desert in New Mexico, USA.
145 *Larrea* is one of the prominent woody encroachers on shallow soils in lowland deserts
146 throughout the southwestern United States. In contrast to mesquite (*Prosopis* spp.), which has
147 encroached into deeper soils, *Larrea* is not capable of symbiotic N₂ fixation. We performed a
148 two pool density separation on a replicated suite of soils from three microsite types typical of an
149 encroachment scenario (remnant intact grassland, shrub subcanopies, and in shrub intercanopy
150 spaces within a shrub-encroached area; n = 3 microsities x 10 replicates = 30), separating soils
151 into commonly-used light fraction (“LF”; particle density <1.85 g cm⁻³) and heavy fraction (“HF”;
152 >1.85 g cm⁻³) pools. Soils were sampled to 10 cm depth under the entire subcanopy area (or 1 x
153 1 m patches for shrub intercanopy spaces and grassland), thus providing an integrated
154 representation of the subcanopy area and embracing expected patterns of sub-canopy spatial
155 variability (Throop and Archer 2008). To further explore how C was distributed with mineral
156 particle density, we fractionated soils from two of the vegetation microsities (intact grassland and

157 shrub subcanopy) into seven different density fractions, ranging in particle density from $<1.65 \text{ g cm}^{-3}$
158 cm^{-3} to $>2.65 \text{ g cm}^{-3}$ (Sollins et al. 2009). The two density fractionation allowed us to conduct a
159 replicated study quantifying differences in C distribution among microsites, while the more costly
160 and labor intensive seven density fractionation provided more detail about C distribution among
161 fractions differing in particle density. For both fractionation techniques, we used stable isotope
162 analyses to assess the contribution of C_3 and C_4 pathways to soil C pools. Our goal was to
163 explore C pools and potential stabilization processes following land cover change in a desert
164 grassland ecosystem.

165

166 **Methods**

167 *Study Location*

168 Soil samples were collected from the Chihuahuan Desert Rangeland Research Center in the
169 northern Chihuahuan Desert (Doña Ana County, New Mexico, USA; $32^{\circ}30'N$, $106^{\circ}47'W$), where
170 shrub establishment into former grassland has occurred over the past 150 years (Gibbens et al.
171 2005). The study site forms part of the National Science Foundation's Jornada Basin Long
172 Term Ecological Research site. The climate is arid (MAP = 245 mm, MAT = 14.7°C), with the
173 majority ($>60\%$) of precipitation occurring as monsoonal thunderstorms between 1 June and 1
174 October (Wainwright 2006). Soils were collected from the upper bajada of Mt. Summerford,
175 where the historically dominant C_4 perennial bunchgrass (black grama, *Bouteloua eriopoda*)
176 has been largely replaced by the evergreen C_3 shrub creosote bush (*Larrea tridentata*) during
177 the past century. Remnant patches of intact black grama grasslands selected for sampling
178 were located slightly upslope, but in close proximity to, areas encroached by creosote bush
179 (*Larrea tridentata*) that were selected for sampling. In areas dominated by creosote bush, shrub
180 interspaces are largely devoid of perennial plants, with the exception of patches of the invasive
181 African grass *Eragrostis lehmanniana*. Areas invaded by *E. lehmanniana* were avoided in the
182 sampling campaigns. Soils at all sites selected for sampling are igneous-derived coarse-loamy

183 alluvium in the Onite-Pajarito association (coarse-loamy mixed superactive thermic Typic
184 Calciargids and Typic Haplocambids). Although historical livestock grazing at the site has been
185 attributed as a primary cause of the grassland to shrubland transition, grazing has been absent
186 from the site since 1982 (Havstad and Schlesinger 2006). Soil sampling focused on surface
187 soils (0-10 and 0-15 cm) as these depths account for a large fraction of soil profile C in deserts
188 (Jobbagy and Jackson 2000). Furthermore, surface soils (<10 cm depth) typically exhibit the
189 most dynamic change in SOC as a response to woody plant establishment or removal in
190 drylands and reported woody encroachment impacts on SOC appear to be typically restricted to
191 < 20 cm depths (Barth and Klemmedson 1978; Boutton et al. 2009; McClaran et al. 2008;
192 Tiedemann and Klemmedson 1986).

193

194 *Density Fractionation*

195 A sampling campaign was conducted in November 2010 to characterize the SOC pool
196 difference in response to *Larrea* encroachment. We selected 10 replicates for each of three
197 vegetation microsites (n = 30). *Larrea* subcanopy (hereafter 'subcanopy') samples were
198 collected under individual *Larrea* shrubs that were representative of the shrubs present at the
199 site: approximately 2.0 m canopy diameter, at least one canopy diameter from the nearest
200 neighboring *Larrea* or other woody plants, and no evidence of recent surface erosion. Shrub
201 subcanopy soils may have strong bole to dripline gradients in SOC (Throop and Archer 2008).
202 To integrate these spatial patterns in SOC across the entire subcanopy area, we collected all
203 the subcanopy soil to 10 cm depth, homogenized it, and retained a 250 g subsample. For the
204 *Larrea* intercanopy (hereafter 'intercanopy') and intact black grama grassland (hereafter
205 'grassland') microsites, we obtained all the soil from a 1 m x 1 m patch, homogenized it, and
206 retained a 250 g subsample. Selected microsite patches were at least one canopy diameter
207 from neighboring *Larrea* canopies and had no evidence of recent surface erosional processes
208 or small mammal activity. Prior to bulk sample collection at each microsite replicate, a

209 volumetric soil core to 10 cm depth was obtained for bulk density calculation. Soils were oven
210 dried at 60°C, passed through a 2 mm sieve, and stored dry until density fractionation. Bulk
211 density was calculated as the mass of the fine earth (<2 mm) fraction divided by the volume of
212 the entire core, thus accounting for volume displaced by >2 mm fragments (Throop et al. 2012).

213

214 Soils were separated into two density fractions using sodium polytungstate (SPT) following the
215 procedures of Sollins *et al.* (2006), using an initial mass of 40 g soil for each microsite sample.
216 Samples were gently shaken in 250 ml centrifuge tubes for 3 h and spun at 1285 rpm for 25
217 min. The floating material and supernatant (hereafter 'LF' for light fraction) were aspirated off.
218 Both LF and the remaining heavy fraction (HF) were rinsed multiple times with deionized water
219 and collected on glass fiber filters (Whatman GF/F). An SPT density of 1.85 g cm⁻³ was used
220 because results from the seven density fractionation (below) suggested that this density
221 provided a clear separation between free organic matter and that bound to mineral particles. We
222 refer to this density separation as the "two density fractionation".

223

224 To explore the density distribution of C in more detail, two soil samples from contrasting
225 microsites (grassland and shrub subcanopy, n = 1 sample/microsite) were subjected to a more
226 detailed SDF procedure that yielded seven density fractions. The shrub subcanopy soil was
227 collected from the edge of a *Larrea* canopy. Approximately 1 kg of soil was collected with a
228 trowel from the top 15 cm of soil profile at each sampling location. An initial mass of 180 g soil
229 for each sample was shaken (1-3 h) with SPT in a 1 L tube, centrifuged at 3000 rpm, and the
230 floating material and supernatant was aspirated off and rinsed. This procedure was repeated
231 with sequentially increasing SPT target densities of 1.65, 1.85, 2.00, 2.20, 2.45, and 2.65 g cm⁻³
232 (actual values ± 0.03 g cm⁻³ of target densities); for expediency we refer to the resulting density
233 fractions by the maximum particle density (e.g. 1.65, 1.85 g cm⁻³). We refer to this sequential
234 density separation as the "seven density fractionation".

235

236 *Analytical Methods*

237 For both density fractionation procedures, samples were dried at 60°C, weighed, and ground
238 using a ball mill. Subsamples of each density fraction and the bulk soil were analyzed in
239 triplicate for C and N concentration on an elemental analyzer (ECS 4010, Costech Analytical,
240 Valencia, CA) at New Mexico State University. A second set of replicate subsamples were acid
241 fumigated prior to CN analysis to remove any carbonates (Harris et al. 2001); carbonate
242 concentration of the soils was calculated from the difference in C concentration between
243 fumigated and non-fumigated samples. Analysis of internal standards indicated an analytical
244 error of <3% for C. In addition to mass-based concentration of C and N of individual fractions
245 (e.g., mg C g⁻¹ of a fraction), C and N concentration of individual fractions relative to bulk soil
246 were calculated from fraction C or N concentration and total fraction mass data (e.g., mg C g⁻¹
247 bulk soil). Samples were analyzed for δ¹³C with a coupled continuous-flow elemental analyzer-
248 isotope ratio mass spectrometer (EA-IRMS) system with a Carlo-Erba model 1108 EA
249 interfaced to a Thermo-Finnigan Delta Plus XP IRMS at the Light Stable Isotope Facility of the
250 University of California, Santa Cruz. ¹³C data are reported relative to the Pee Dee Belemnite
251 (PDB) standard. Precision of in-house standards, which had been calibrated using international
252 standards, was typically better than 0.2 per mil for δ¹³C. One standard was run for every ten
253 unknowns, and two blanks and conditioning and calibration standards were included at the
254 beginning and end of each run. Samples were run in duplicate and were always within the range
255 of the standards.

256

257 Statistical analyses on the two density fractionation samples were performed in JMP 7.0.1 (SAS
258 Institute, Cary, NC). One-way ANOVA procedures were used to test for among-vegetation
259 microsite differences in response variables. LF, HF, and bulk pools were analyzed separately.
260 Significance of differences among means were assessed with a *post hoc* Student-Newman-

261 Kuels test. No statistical analyses were performed on the seven density fractionation samples
262 due to lack of replication.

263

264 **Results**

265 *Carbon and Nitrogen Pools*

266 Organic C concentrations in the bulk soil samples differed among vegetation microsites, with
267 shrub subcanopy soils averaging nearly twice that of grassland soils and nearly three times that
268 of shrub intercanopy soils (Figure 1; $F_{2,27} = 10.40$, $P = 0.0004$). Bulk soils also differed in
269 concentration of inorganic C as CaCO_3 ($F_{2,27} = 9.08$, $P = 0.001$), with essentially no carbonates
270 in grasslands and on average nearly twice as much carbonate C in intercanopy soils as in
271 subcanopy soils (1.58 ± 0.412 and 0.84 ± 0.240 mg $\text{CaCO}_3\text{-C g}^{-1}$ bulk soil, respectively; mean \pm
272 SE). Consequently, total C (organic + inorganic) concentration was significantly greater in the
273 shrub subcanopy than the two other microsites (Figure 1; $F_{2,27} = 8.00$, $P = 0.0019$). Bulk density
274 was significantly greater in the two shrub microsites (subcanopy: 0.98 ± 0.031 , intercanopy:
275 0.99 ± 0.026 g cm^{-3}) than the grassland (0.83 ± 0.035 g cm^{-3} ; $F_{2,27} = 8.76$, $P = 0.001$),
276 magnifying the difference in C among microsites when total C was expressed on an areal basis
277 (326 ± 28.9 , 236 ± 14.5 , and 662 ± 113.8 g C m^{-2} to 10 cm depth for grassland, intercanopy, and
278 subcanopy, respectively; $F_{2,27} = 10.76$, $P = 0.0004$).

279

280 Patterns of C in the two density fractionation study were strongly affected by vegetation
281 microsite. There was proportionally less LF dry mass in the shrub intercanopy microsite than
282 the other two microsites ($F_{2,27} = 6.42$, $P = 0.005$), although there was no difference in organic C
283 concentration of the LF among microsites ($F_{2,27} = 0.41$, $P = 0.67$). Consequently, the
284 concentration of LF organic C in the bulk soil (mg LF C g^{-1} bulk soil) was significantly greater in
285 the subcanopy than the intercanopy microsite (Figure 2; $F_{2,27} = 7.00$, $P = 0.004$). For the HF,
286 proportional dry mass was greater in the intercanopy than subcanopy ($F_{2,27} = 3.43$, $P = 0.047$)

287 and organic C concentration of the HF was lower in the intercanopy than the other two
288 microsities ($F_{2,27} = 5.93$, $P = 0.007$). Consequently, the concentration of HF organic C in the bulk
289 soil (mg HF C g^{-1} bulk soil) was significantly lower in the intercanopy than the other two
290 microsities (Figure 2; $F_{2,27} = 5.96$, $P = 0.007$). More soluble organic C was mobilized by SPT in
291 shrub subcanopy soils than in the other two soils (Figure 2; $F_{2,27} = 9.43$, $P = 0.0008$), and this
292 was roughly equal in magnitude to HF C in shrub subcanopy soils. Pedogenic carbonates were
293 found in significant quantities in the two shrub microsite soils but not in the grassland soils ($F_{2,27}$
294 $= 3.67$, $P = 0.039$), with means trending higher in intercanopy soils than in shrub subcanopy
295 soils. Trends in soil N concentration followed those of soil organic C (Figure 3a; LF: $F_{2,27} = 7.59$,
296 $P = 0.002$; HF: $F_{2,27} = 4.83$, $P = 0.016$). Organic C:N of LF grassland soils was significantly
297 greater than organic C:N of either subcanopy or intercanopy shrub LF soils (Figure 3b; $F_{2,27} =$
298 19.51 , $P < 0.0001$), while organic C:N decreased from grassland to subcanopy to intercanopy
299 (Figure 3b; $F_{2,27} = 14.93$, $P = 0.001$).

300
301 Results from the seven density fractionation provide further insight into differences in C
302 distribution and stabilization between the grassland and shrub subcanopy. For the two lightest
303 fractions (1.65 and 1.85 g cm^{-3}), organic C concentration (mg C g^{-1} bulk soil) was greater in the
304 shrub subcanopy soil than in grassland soil (Figure 4a). For all heavier density fractions,
305 organic C was similar between the two microsities (Figure 4a). However, C:N patterns of density
306 fractions were more complex (Figure 4b). In the two density fractionation, LF C:N of grassland
307 soils was greater than that of the shrub subcanopy soils (Figure 3b). The seven density
308 fractionation illustrated that C:N in the LF was driven by the 1.85 g cm^{-3} fraction rather than the
309 1.65 g cm^{-3} fraction (Figure 4b). Similarly, while C:N of HFs in the two density fractionation were
310 similar between grass and shrub subcanopy sites, C:N of specific heavy density fractions in the
311 seven density fractionation differed.

312

313 *Stable Isotopes*

314 The bulk shrub subcanopy soil was depleted in $\delta^{13}\text{C}$ relative to the bulk grassland soil (-20.54‰
315 and -18.17‰, respectively). In the two density fractionation, both LF and HF were depleted of
316 $\delta^{13}\text{C}$ in shrub subcanopy microsites relative to grassland microsites (Figure 5; LF: $F_{2,27} = 40.75$,
317 $P < 0.0001$; HF: $F_{2,27} = 13.24$, $P < 0.0001$). LF of intercanopy soils was intermediate between
318 grassland and shrub subcanopy values, while HF values of intercanopy soils did not differ
319 significantly from shrub subcanopy soils. Data from the seven density fractionation showed that
320 all density fractions of the shrub subcanopy soil were ^{13}C depleted compared to the grassland
321 soil (Figure 6). For the lightest fraction, the subcanopy soil was depleted in $\delta^{13}\text{C}$ relative to the
322 grassland soil by 4.9‰. For all other fractions, the subcanopy soil was depleted relative to the
323 grassland by approximately 1‰. Both soils exhibited a general increase in $\delta^{13}\text{C}$ with increasing
324 fraction density until the 2.45 g cm^{-3} fraction, followed by substantial declines in $\delta^{13}\text{C}$ in the two
325 densest fractions, such that the densest fraction was more depleted in $\delta^{13}\text{C}$ than C_3 *Larrea*
326 leaves and leaf litter (-24.6‰ and -24.8‰ for leaves and litter, respectively; Rasmussen and
327 White 2010).

328

329 ***Discussion***

330 *Grass and Shrub Contributions to C Pools*

331 Increases in SOC under shrubs at our study site are congruent with the well-described island of
332 fertility effect (Garcia-Moya and McKell 1970) that sometimes includes losses of C from
333 intercanopy soils following shrub encroachment (Schlesinger et al. 1990). While we report our
334 results primarily on a per mass basis, greater bulk density in the shrub microsites magnify the
335 positive impact of shrubs on areally-based C estimates. Both density fractionation techniques
336 suggest that increases in C under shrubs are driven by light fractions composed of plant debris
337 and entrained mineral material. In contrast, C in the heavy fractions remained essentially
338 unchanged between the subcanopy and grassland vegetation microsites. Although *P*.

339 *glandulosa* encroachment led to increases in particulate organic matter C within a few decades
340 of encroachment in south Texas, accumulation of C in more stabilized macroaggregates
341 increased dramatically, but only in stands < 80 y old (Liao et al. 2006b). Incorporation of C into
342 heavy fractions may likewise occur in the future following continued growth and organic inputs
343 from *Larrea*. Our stable isotope data suggest that while the heavy fraction C concentration
344 remains quite static relative to vegetation change, the isotopic composition of all fractions,
345 including the heavy ones, show shifts in isotopic signature consistent with C₃ inputs into these
346 pools. Thus, even the heavy fractions, which are thought to be most stabilized (Sollins et al.
347 2009), appear to have dynamic inputs and outputs of recently-derived organic material.

348

349 Although the concentration of C in our dryland study system is quite low, the magnitude and rate
350 of change in SOC in response to woody encroachment were quite high. Shrub subcanopy
351 microsites averaged 335 g C m⁻² more than grassland sites, while shrub intercanopy sites
352 averaged 90 g C m⁻² less than grassland sites. Assuming that encroachment at this site
353 occurred in the last 70 years (Gibbens et al. 2005) and linear C accumulation under shrubs
354 through time, we estimate a subcanopy accumulation rate of 4.8 g C m⁻² y⁻¹ (to 10 cm depth). If
355 *Larrea* canopies account for 50% of the land area (Rango et al. 2005), landscape-level
356 accumulation (subtracting out losses in intercanopy areas) would be 1.75 g C m⁻² y⁻¹. These
357 values are much lower than values reported for N-fixing *Prosopis glandulosa* in south Texas
358 (10–30 g C m⁻² y⁻¹ to 15 cm depth; Liao et al. 2006b) or *P. velutina* in the Sonoran Desert (12 g
359 m⁻² yr⁻¹ to 20 cm depth; Wheeler et al. 2007). However, Throop and Archer (2008) point out that
360 single-point sampling under shrub canopies can drastically overestimate rates of C
361 accumulation, and suggest that C accumulates under *P. velutina* in the Sonoran Desert at only
362 2.6 g C m⁻² y⁻¹ to 20 cm depth when spatial patterns are taken into account. Our method of
363 sampling all the subcanopy soil integrates across the entire canopy area, and thus is most
364 equivalent to the Throop and Archer (2008) estimate. This would translate into a substantial flux

365 of C if similar patterns are found in the >19 million ha of southwestern North America where
366 *Larrea* is the dominant shrub (Van Auken 2000).

367
368 Stable isotope analyses can be used to characterize the contribution of plants with C₃ and C₄
369 photosynthetic pathways to soil C pools, and woody expansion in southwestern US drylands
370 have been particularly amenable to these analyses due to C₃ shrub encroachment into former
371 C₄ grasslands (Boutton et al. 1998). Woody encroachment at our study site leads to an
372 approximate -2‰ shift in δ¹³C for bulk soils, similar to that caused by small *Prosopis velutina*
373 shrubs encroaching into Sonoran Desert grasslands (Wheeler et al. 2007) but smaller than the -
374 3‰ to -6‰ shift following *P. glandulosa* encroachment in Texas (Liao et al. 2006a). However,
375 although our soil collection locations in the remnant C₄ grasslands were devoid of C₃ shrubs in
376 close proximity, δ¹³C of bulk grassland soils (-18.2‰) was depleted in ¹³C relative to C₄ grass
377 inputs (-14.2‰). This ¹³C depletion can not be explained by isotopic fractionation during SOM
378 formation, as SOM is typically ¹³C enriched due to preferential respiration of light ¹²C (Ehleringer
379 et al. 2000). Scattered C₃ shrubs, annual C₃ forbs present in high favorable precipitation years,
380 or erosional inputs from C₃ shrubs found upslope (e.g., *Juniperous* and *Quercus*) may account
381 for this. Alternatively, low ¹³δC values may reflect disproportionate retention of organic
382 compounds such as lignin that are typically depleted in ¹³C (Benner et al. 1987).

383
384 Increases in δ¹³C with increasing density fraction (up to the 2.45 g cm⁻³ fraction) are consistent
385 with previous observations that have been interpreted as fractionation during microbial
386 processing, although the dramatic drop in δ¹³C in the two heaviest fractions has not been
387 reported in other studies (Dijkstra et al. 2006; Sollins et al. 2009). Residual CaCO₃ following
388 acid fumigation is not an explanation, as the isotopic signature of CaCO₃ is relatively enriched in
389 ¹³C (Monger et al. 2009). The low δ¹³C could reflect a disproportionate retention of material with
390 low δ¹³C or an unknown fractionation source that preferentially removed ¹³C. With respect to

391 the first possibility, the two heaviest pools may be enriched in lignin, which is generally depleted
392 in ^{13}C relative to bulk litter (Benner et al. 1987). However, while lignin is relatively resistant to
393 decay in surface litters (e.g., Meentemeyer 1978), recent studies suggest that it is not
394 preferentially preserved in soils and exerts little influence on the stability of mineral-associated
395 soil fractions (reviewed in Thevenot et al. 2010). Furthermore, C stabilized onto mineral
396 fractions generally has an isotopic signature more similar to microbially processed organic
397 matter than to plant compounds (Grandy and Neff 2008; Kiem and Kögel-Knabner 2003).
398

399 Isotope mixing models are used on bulk soils and, increasingly, following physical or density
400 separation techniques, to assess the relative contribution of C_3 and C_4 sources to SOC pools,
401 but our results reveal some difficulties in model interpretation posed by fractionation during
402 SOM formation. Ideally we would have a pure C_4 grassland soil and a C_3 shrub soil with no
403 previous C_4 history to serve as mixing model end-members. Such pure end-members can be
404 obtained in controlled cropping systems, yet are rare in natural systems, and thus plant isotopic
405 signatures are generally used as at least one, if not both, end-members in mixing models.
406 However, SOM is generally 2-5‰ $\delta^{13}\text{C}$ isotopically heavier than plant inputs due to fractionation
407 during decomposition (Krull et al. 2002; Stevenson et al. 2005); isotopic differences among our
408 seven density fractions suggest such fractionation. To estimate the C_3 and C_4 contribution to
409 SOC, we used the lightest fraction material from the grassland and shrub subcanopy. This end-
410 member mixing model suggests that roughly 50% shrub subcanopy C is derived from C_3 inputs.
411 Calculating contributions to stable heavier fraction C is more complex. The large clay-rich
412 fraction (2.45 g cm^{-3}) in the grassland was enriched by 1.6‰ compared to the lightest fraction.
413 Assuming that the same fractionation would occur for a pure shrub signal, we calculated that
414 heavy fraction C in the shrub subcanopy reflects a 70% contribution of residual C_4 -C. These
415 rough calculations suggest input of C_3 material into both labile and more stable C pools.

416

417 *Comparison with Soils from More Mesic Environments*

418 To gain insight into differences between processes in drylands and better studied mesic
419 systems, we compared our seven density fractionation results with a broader survey of soils
420 from more mesic environments reported in Sollins et al. (2009). As expected, organic C in our
421 desert soils was low compared to more mesic and forested ecosystems (Figure 7a). Jornada
422 shrub subcanopy soils had a higher percent of total C in the lightest fraction (41%) than the
423 other soils, and the Jornada grassland had as high a percent of C in the lightest fraction material
424 (33%) as the highest forests measured. While mineralogy and clay content may drive some of
425 these differences (Torn et al. 1997), climate controls on litter vs. SOM decomposition processes
426 may also play a role. The tropical dry forest shows a relatively small proportion of C in the
427 lightest fraction; this suggests that the desert soils have conditions more favorable for SOM
428 degradation or else that a greater proportion of desert litter decomposes efficiently to CO₂ and is
429 not stabilized in soil heavy fractions. The low root biomass and seasonally low root activity
430 likely lead to lower aggregate stabilization in drylands, and indeed, the dryland soils were
431 unique in not having spikes in C in the 1.85-2.4 g cm⁻³ fractions, which are typically dominated
432 by aggregates (Hatton et al. 2012). The isotopic composition of our dryland soils differed
433 strikingly from previously studied mesic and forested ecosystems, suggesting differences both
434 in input source and SOM stabilization processes. Except for the heaviest fraction, the dryland
435 soils were considerably enriched in ¹³C relative to the other soils due to significant C₄ plant
436 inputs (Figure 7b). While all soils follow the pattern of ¹³C enrichment with increasing density in
437 the lighter fractions, the dramatic ¹³C depletion of the two heaviest fractions is particularly
438 striking given that this pattern occurred only in the dryland soils.

439

440 *Dryland Soluble C Pools*

441 Many density fraction studies using SPT have noted losses of particulate or soluble C during the
442 fractionation procedure. Kramer et al. (2009) reported losses of under 8% for several soils

443 during an overnight soaking experiment in SPT, perhaps due to particulate loss during the
444 fractionation procedure. Indeed, Crow et al. (2007) reported larger losses of C (mean = 20%)
445 from the same Pacific Northwest coniferous soils after a larger-scale density fractionation,
446 perhaps due to the greater number of steps involved during that experiment. However, patterns
447 of C loss in our two density fractionation with SPT appear to be too great to be attributable to
448 laboratory particulate losses during a single density separation, and the microsite pattern of
449 soluble C loss suggests an alternate, more ecologically meaningful explanation. Because the
450 largest soluble C losses occurred in shrub subcanopy soils (35% of total C on a per mass basis
451 versus 2-4% in grass or intercanopy soils), we hypothesize that microbial activity and root
452 exudation during periods where soils are drying, but still wet enough for biotic activity, lead to
453 the build-up of soluble organic acids in surface soils. With the onset of rain, these products are
454 likely mobilized or respired. Results of the Crow et al. (2007) study might also reflect stores of
455 soluble C, as these soils were collected during the prolonged summer dry season in the Pacific
456 Northwest. An alternative explanation, that C losses were composed of residual CaCO_3 , is
457 unlikely due to both isotopic results (reported $\delta^{13}\text{C}$ of CaCO_3 is -12 to +2‰ at our study site;
458 Monger et al. 2009) and the disparity between the distribution of CaCO_3 and SPT soluble C
459 among vegetation microsites. Support for our hypothesis of a soluble, perhaps seasonal, C pool
460 comes from studies of streamwater chemistry in ecosystems with marked seasonality of
461 precipitation where increased DOC flushes occur during rains following dry periods (Brooks et
462 al. 2007; van Verseveld et al. 2009; Vanderbilt et al. 2003), also likely due to a build up of small
463 organic molecules as soils are drying. The existence of a pool of potentially mobilized SOC in
464 drylands has significant implications for our understanding of mechanisms of SOC stabilization.

465

466 *Dryland Carbonate C Pools*

467 Carbonates are a significant C pool both locally and globally, with soil carbonates accounting for
468 the third largest pool in the global C cycle (Schlesinger 1997). Results from this study of

469 surface soils indicate microsite differences in carbonates, with shrub intercanopy soils having
470 greater carbonate concentration than grasslands or shrub subcanopies. Given the same parent
471 material for all soils, we hypothesize that greater carbonates in intercanopy soils is related to
472 erosion of surface horizons (Wilcox et al. 1996) rather than to microsite differences in carbonate
473 formation. Our estimates of bulk SOC changes suggest that accumulation rates under *Larrea*
474 canopies ($4.79 \text{ g C m}^{-2} \text{ y}^{-1}$) are greater than carbonate accumulation rates ($0.012 - 1.3 \text{ g C m}^{-2}$
475 yr^{-1} ; Monger and Martinez-Rios 2000), and SOC accumulation rates are likely greater than
476 carbonates even when intercanopy SOC losses are accounted for ($1.75 \text{ g C m}^{-2} \text{ y}^{-1}$).

477

478 *Conceptual Model of Dryland Soil Carbon*

479 Models of SOM dynamics have used different numbers of pools, defined in different ways, to
480 represent fractions of organic matter that are chemically or biophysically distinct and have
481 different turnover rates, even when it is generally acknowledged that turnover times and pools
482 are likely continuous, not discrete. For example, the CENTURY model has been widely used to
483 represent soil C pools based on three compartments for SOM (active, slow and passive) with
484 different potential decomposition rates defined on a theoretical basis rather than experimentally
485 (Parton et al. 1993; Parton et al. 1988). Hatton et al. (2012) built on this conceptual framework,
486 proposing a similar model for forest SOM based on density fractions. Their model contains a
487 light fraction composed of plant fragments not associated with minerals (equivalent to our LF),
488 aggregates or organic matter associated with light clays ($1.85\text{-}2.4 \text{ g.cm}^{-3}$), and primary mineral
489 particles coated with pedogenic oxides and patches of organic matter ($>2.4 \text{ g cm}^{-3}$). This model
490 provides a testable and simple framework for understanding soil C pools and their dynamics.

491

492 Results from our study suggest that two other pools should be added to this conceptual model
493 in dryland ecosystems: the seasonally soluble pool and carbonates (Figure 8). We expect all
494 five pools to vary considerably among dryland ecosystems that differ in climate and vegetative

495 regimes, and also we expect that local spatial heterogeneity will generally increase dramatically
496 in these pools with conversion of grassland to shrubland, as we found in this study. In this
497 model, light fraction and root exudate material can decompose into a soluble, but not mobilized
498 pool, in soil or can contribute to aggregate or mineral-associated C. Aggregate and organo-
499 mineral complexes together comprise a heavy fraction ($>1.85 \text{ g cm}^{-3}$) pool, and it may be
500 difficult to draw clear distinctions between these pools.

501

502 In our study, the soluble pool and the light fraction pools both increased with woody
503 encroachment, suggesting that woody encroachment at in this system has significant impacts
504 on short-term C dynamics. Increases in carbonate-C with woody encroachment may reflect
505 increased erosion of surface soils with the loss of grasses, while changes in the isotopic
506 composition of the heavy fraction indicate that this fraction reflects dynamic inputs and outputs.
507 Understanding the processes and rates of C stabilization in drylands are crucial for estimating
508 the current and future dynamics of C pools in globally extensive drylands, particularly in light of
509 dramatic land cover changes due to woody encroachment and the current uncertainty of the role
510 of this land cover change as a terrestrial C sink.

511

512 **Acknowledgements**

513 We greatly appreciate advice, ideas, and laboratory expertise from P. Sollins and assistance
514 from C. Laney, D. Hewins, H. Lee, J. Smith, J. Throop, and J. Wigg. Thoughtful comments from
515 two reviewers improved this manuscript. Financial support for this work was provided by the
516 National Science Foundation (DEB 0817064 to KL, DEB 0953864 to HT) and USDA-NRI
517 Managed Ecosystems (2005-35101-15408 to S. Archer, HT, and M. McClaran). The Jornada
518 Basin LTER is supported by NSF DEB 0618210.

519 **Literature Cited**

- 520 Amundson R (2001) The carbon budget in soils. *Annu Rev Earth Pl Sc* 29:535–562
- 521 Archer S (1994) Woody plant encroachment into southwestern grasslands and savannas: rates,
522 patterns and proximate causes. In: Vavra M, Laycock WA, Pieper RD (eds) *Ecological*
523 *implications of livestock herbivory in the West*. Society for Range Management, Denver,
524 CO, pp 13-68
- 525 Archer S (1995) Tree-grass dynamics in a *Prosopis*-thornscrub savanna parkland:
526 Reconstructing the past and predicting the future. *Ecoscience* 2:83-99
- 527 Archer S, Boutton T, Hibbard K (2001) Trees in grasslands: biogeochemical consequences of
528 woody plant expansion. In: Schultz E, Harrison S, Heiman M et al. (eds) *Global*
529 *Biogeochemical Cycles in the Climate System*. Academic Press, San Diego, pp 115-137
- 530 Bailey RG (1996) *Ecosystem Geography*. Springer, New York
- 531 Baisden WT, Amundson R, Cook AC, Brenner DL (2002) Turnover and storage of C and N in
532 five density fractions from California annual grassland surface soils. *Global Biogeochem*
533 *Cy* 16:1117. doi:10.1029/2001GB001822
- 534 Barger NN, Archer SR, Campbell JL, Huang CH, Morton JA, Knapp AK (2011) Woody plant
535 proliferation in North American drylands: a synthesis of impacts on ecosystem carbon
536 balance. *J Geophys Res - Biogeo* 116:G00K07
- 537 Barth RC, Klemmedson JO (1978) Shrub-induced spatial patterns of dry matter, nitrogen, and
538 organic carbon. *Soil Sci Soc Am J* 42:804-809
- 539 Belsky AJ, Amundson RG, Duxbury JM, Riha SJ, Ali AR, Mwonga SM (1989) The effects of
540 trees on their physical, chemical, and biological environments in a semi-arid savanna in
541 Kenya. *J Appl Ecol* 26:1005-1024
- 542 Benner R, Fogel ML, Sprague EK, Hodson RE (1987) Depletion of ¹³C in lignin and its
543 implications for stable carbon isotope studies. *Nature* 329:708-710

544 Boutton TW, Archer SR, Midwood AJ, Zitzer SF, Bol R (1998) $\delta^{13}\text{C}$ values of soil organic carbon
545 and their use in documenting vegetation change in a subtropical savanna ecosystem.
546 *Geoderma* 82:5-41

547 Boutton TW, Liao JD, Filley TR, Archer SR (2009) Belowground carbon storage and dynamics
548 accompanying woody plant encroachment in a subtropical savanna. In: Lal R, Follett R
549 (eds) *Soil Carbon Sequestration and the Greenhouse Effect*. 2nd edition edn. Soil
550 Science Society of America, Madison, WI, pp 181-205

551 Brooks PD, Haas PA, Huth AK (2007) Seasonal variability in the concentration and flux of
552 organic matter and inorganic nitrogen in a semiarid catchment, San Pedro River,
553 Arizona. *Journal of Geophysical Research* 112:G03S04. doi:10.1029/2006jg000275

554 Christensen BT (2002) Physical fractionation of soil and structural and functional complexity in
555 organic matter turnover. *Eur J Soil Sci* 52:345-353

556 Crow SE, Swanston C, Lajtha K, Brooks JR, Keirstead H (2007) Density fractionation of forest
557 soils: Methodological questions and interpretation of incubation results and turnover time
558 in an ecosystem context. *Biogeochemistry* 85:69-90

559 Dijkstra P, Ishizu A, Doucett R, Hart S, Schwartz E, Menyailo O, Hungate B (2006) ^{13}C and ^{15}N
560 natural abundance of the soil microbial biomass. *Soil Biol Biochem* 38:3257–3266.
561 doi:10.1016/j.soilbio.2006.04.005

562 Diochon AC, Kellman L (2009) Physical fractionation of soil organic matter: Destabilization of
563 deep soil carbon following harvesting of a temperate coniferous forest. *Journal of*
564 *Geophysical Research* 114:G01016

565 Ehleringer JR, Buchmann N, Flanagan LB (2000) Carbon isotope ratios in belowground carbon
566 cycle processes. *Ecol Appl* 10:412-422

567 Eldridge DJ, Bowker MA, Maestre FT, Roger E, Reynolds JF, Whitford WG (2011) Impacts of
568 shrub encroachment on ecosystem structure and functioning: towards a global
569 synthesis. *Ecol Lett* 14:709-722. doi:doi: 10.1111/j.1461-0248.2011.01630.x

570 Field C, Behrenfeld M, Randerson J, Falkowski P (1998) Primary production of the biosphere:
571 integrating terrestrial and oceanic components. *Science* 281:237-240

572 Garcia-Moya E, McKell CM (1970) Contributions of shrubs to the nitrogen economy of a desert
573 wash plant community. *Ecology* 51:81-88

574 Gibbens RP, McNeely RP, Havstad KM, Beck RF, Nolen B (2005) Vegetation changes in the
575 Jornada Basin from 1858 to 1998. *J Arid Environ* 61:651-668

576 Grandy AS, Neff JC (2008) Molecular C dynamics downstream: The biochemical decomposition
577 sequence and its impact on soil organic matter structure and function. *Sci Total Environ*
578 404:297-307. doi:10.1016/j.scitotenv.2007.11.013

579 Harris D, Horwath WR, van Kessel C (2001) Acid fumigation of soils to remove carbonates prior
580 to total organic carbon or carbon-13 isotopic analysis. *Soil Sci Soc Am J* 65:1853-1856

581 Hatton P-J, Kleber M, Zeller B, Moni C, Plante AF, Townsend K, Gelhaye L, Lajtha K, Derrien D
582 (2012) Transfer of litter-derived N to soil mineral–organic associations: Evidence from
583 decadal ¹⁵N tracer experiments. *Org Geochem* 42:1489-1501.
584 doi:10.1016/j.orggeochem.2011.05.002

585 Havstad KM, Schlesinger WH (2006) Introduction. In: Havstad KM, Huenneke LF, Schlesinger
586 WH (eds) *Structure and Function of a Chihuahuan Desert ecosystem: the Jornada Basin*
587 *Long-Term Ecological Research Site*. Oxford University Press, New York, pp 3-14

588 Hibbard KA, Archer S, Schimel DS, Valentine DW (2001) Biogeochemical changes
589 accompanying woody plant encroachment in a subtropical savanna. *Ecology* 82:1999-
590 2011

591 Jackson R, Canadell J, Ehleringer J, Mooney H, Sala O, Schulze E (1996) A global analysis of
592 root distributions for terrestrial biomes. *Oecologia* 108:389-411

593 Jobbagy E, Jackson R (2000) The vertical distribution of soil organic carbon and its relation to
594 climate and vegetation. *Ecol Appl* 10:423-436

595 Kane ES, Valentine DW, Schuur EAG, Dutta K (2005) Soil carbon stabilization along climate
596 and stand productivity gradients in black spruce forests of interior Alaska. *Can J For Res*
597 35:2118-2129

598 Kiem R, Kögel-Knabner I (2003) Contribution of lignin and polysaccharides to the refractory
599 carbon pool in C-depleted arable soils. *Soil Biol Biochem* 35:101-118

600 Knapp AK, Briggs JM, Collins SL, Archer SR, Bret-Harte MS, Ewers BE, Peters DP, Young DR,
601 Shaver GR, Pendall E, Cleary MB (2008) Shrub encroachment in North American
602 grasslands: shifts in growth form dominance rapidly alters control of ecosystem carbon
603 inputs. *Glob Change Biol* 14:615-623. doi:10.1111/j.1365-2486.2007.01512.x

604 Kramer MG, Lajtha K, Thomas G, Sollins. P (2009) Contamination effects on soil density
605 fractions from high N or C content sodium polytungstate. *Biogeochemistry* 92:177-181

606 Krull ES, Bestland EA, Gates WP (2002) Soil organic matter decomposition and turnover in a
607 tropical ultisol: evidence from $\delta^{13}\text{C}$, $\delta^{15}\text{N}$ and geochemistry. *Radiocarbon* 44:93-112

608 Lajtha K, Schlesinger WH (1986) Plant response to variations in nitrogen availability in a desert
609 shrubland community. *Biogeochemistry* 2:29-37

610 Lal R (2004) Carbon sequestration in dryland ecosystems. *Environ Manag* 33:528-544

611 Liao JD, Boutton TW, Jastrow JD (2006a) Organic matter turnover in soil physical fractions
612 following woody plant invasion of grassland: Evidence from natural ^{13}C and ^{15}N . *Soil Biol*
613 *Biochem* 38:3197-3210

614 Liao JD, Boutton TW, Jastrow JD (2006b) Storage and dynamics of carbon and nitrogen in soil
615 physical fractions following woody plant invasion of grassland. *Soil Biol Biochem*
616 38:3184-3196

617 McClaran MP, Moore-Kucera J, Martens DA, van Haren J, Marsh SE (2008) Soil carbon and
618 nitrogen in relation to shrub size and death in a semi-arid grassland. *Geoderma* 148:60-
619 68

620 McLauchlan KK, Hobbie SE (2004) Comparison of labile soil organic matter fractionation
621 techniques. *Soil Sci Soc Am J* 68:1616-1625

622 Meentemeyer V (1978) Macroclimate and lignin control of litter decomposition rates. *Ecology*
623 59:465-472

624 Monger HC, Cole DR, Buck BJ, Gallegos RA (2009) Scale and the isotopic record of C4 plants
625 in pedogenic carbonate: from the biome to the rhizosphere. *Ecology* 90:1498-1511.
626 doi:10.1890/08-0670.1

627 Monger HC, Martinez-Rios JJ (2000) Inorganic carbon sequestration in grazing lands. In: Follett
628 RF, Kimble JM, Lal R (eds) *The Potential of U.S. Grazing Lands to Sequester Carbon*
629 *and Mitigate the Greenhouse Effect*. Lewis Publishers, Boca Raton, pp 87-118

630 Okin GS, Gillette DA (2001) Distribution of vegetation in wind-dominated landscapes:
631 Implications for wind erosion modeling and landscape processes. *Journal of*
632 *Geophysical Research* 106(D9):9673-9684

633 Pacala SW, Hurtt GC, Baker D, Peylin P, Houghton RA, Birdsey RA, Heath L, Sundquist ET,
634 Stallard RF, Ciais P, Moorcroft P, Caspersen JP, Shevliakova E, Moore B, Kohlmaier G,
635 Holland E, Gloor M, Harmon ME, Fan S-M, Sarmiento JL, Goodale CL, Schimel D, Field
636 CB (2001) Consistent land- and atmosphere-based U.S. carbon sink estimates. *Science*
637 292:2316-2320

638 Parton WJ, Scurlock JMO, Ojima DS, Gilmanov TG, Scholes RJ, Schimel DS, Kirchner T,
639 Menaut J-C, Seastedt T, Gardia Moya E, Kamnalrut A, Kinyumario JI (1993) Observations
640 and modeling of biomass and soil organic matter dynamics for the grassland biome
641 worldwide. *Global Biogeochem Cy* 7:785-809

642 Parton WJ, Stewart JWB, Cole CV (1988) Dynamics of C, N, P and S in grassland soils: a
643 model. *Biogeochemistry* 5:109-131

644 Rango A, Huenneke L, Buonopane M, Herrick JE, Havstad KM (2005) Using historic data to
645 assess effectiveness of shrub removal in southern New Mexico. *J Arid Environ* 62:75-91

646 Rasmussen C, White DA, II (2010) Vegetation effects on soil organic carbon quality in an arid
647 hyperthermic ecosystem. *Soil Sci* 175:438-446

648 Schlesinger WH (1997) *Biogeochemistry: An Analysis of Global Change*. 2nd edn. Academic
649 Press, San Diego

650 Schlesinger WH, Reynolds JF, Cunningham GL, Huenneke LF, Jarrell WM, Virginia RA,
651 Whitford WG (1990) Biological feedbacks in global desertification. *Science* 247:1043-
652 1048

653 Sollins P, Kramer MG, Swanston C, Lajtha K, Filley T, Aufdenkampe AK, Wagai R, Bowden R
654 (2009) Sequential density fractionation across soils of contrasting mineralogy: evidence
655 for both microbial- and mineral-controlled soil organic matter stabilization.
656 *Biogeochemistry* 96:209-231

657 Sollins P, Swanston C, Kleber M, Filley T, Kramer M, Crow S, Caldwell BA, Lajtha K, Bowden R
658 (2006) Organic C and N stabilization in a forest soil: Evidence from sequential density
659 fractionation. *Soil Biol Biochem* 38:3313-3324

660 Stevenson BA, Kelly EF, McDonald EV, Busacca AJ (2005) The stable carbon isotope
661 composition of soil organic carbon and pedogenic carbonates along a bioclimatic
662 gradient in the Palouse region, Washington State, USA. *Geoderma* 124:37-47

663 Thevenot M, Dignac M-F, Rumpel C (2010) Fate of lignins in soils: A review. *Soil Biol Biochem*
664 42:1200-1211

665 Throop HL, Archer SR (2007) Interrelationships among shrub encroachment, land management,
666 and leaf litter decomposition in a semi-desert grassland. *Ecol Appl* 17:1809-1823

667 Throop HL, Archer SR (2008) Shrub (*Prosopis velutina*) encroachment in a semi-desert
668 grassland: spatial-temporal changes in soil organic carbon and nitrogen pools. *Glob*
669 *Change Biol* 14:2420-2431

670 Throop HL, Archer SR, Monger HC, Waltman SW (2012) When bulk density methods matter:
671 Implications for estimating soil organic carbon pools in coarse soils. *J Arid Environ*
672 77:66-71. doi:10.1016/j.jaridenv.2011.08.020

673 Tiedemann AR, Klemmedson J (1986) Long-term effects of mesquite removal on soil
674 characteristics: I. Nutrients and bulk density. *Soil Sci Soc Am J* 50:472-475

675 Torn MS, Trumbore SE, Chadwick OA, Vitousek PM, Hendricks DM (1997) Mineral control of
676 soil organic carbon storage and turnover. *Nature* 389:170-173

677 Trumbore S (2000) Age of soil organic matter and soil respiration: radiocarbon constraints on
678 belowground dynamics. *Ecol Appl* 10:399-411. doi:10.1890/1051-
679 0761(2000)010[0399:AOSOMA]2.0.CO;2

680 Trumbore SE, Davidson EA, Camargo PBd, Nepstad DC, Martinelli LA (1995) Belowground
681 cycling of carbon in forests and pastures of eastern Amazonia. *Global Biogeochem Cy*
682 9:515-528

683 Van Auken OW (2000) Shrub invasions of North American semiarid grasslands. *Annu Rev Ecol*
684 *Syst* 31:197-215

685 van Verseveld WJ, McDonnell JJ, Lajtha K (2009) The role of hillslope hydrology in controlling
686 nutrient loss. *J Hydrol* 367:177-187

687 Vanderbilt KL, Lajtha K, Swanson F (2003) Biogeochemistry of unpolluted forested watersheds
688 in the Oregon Cascades: temporal patterns of precipitation and stream nitrogen fluxes.
689 *Biogeochemistry* 62:87-117

690 Wainwright J (2006) Climate and climatological variations in the Jornada Basin. In: Havstad KM,
691 Huenneke LF, Schlesinger WH (eds) *Structure and Function of a Chihuahuan Desert*
692 *Ecosystem*. Oxford University Press, Oxford, pp 44-80

693 Weltz MA, Kidwell MR, Fox HD (1998) Influence of abiotic and biotic factors in measuring and
694 modeling soil erosion on rangelands: State of knowledge. *J Range Manag* 51:482-495

695 Wessman C, Archer S, Johnson L, Asner G (2004) Woodland expansion in US grasslands:
696 assessing land-cover change and biogeochemical impacts. In: Gutman G, Janetos AC,
697 Justice CO et al. (eds) Land Change Science: Observing, Monitoring and Understanding
698 Trajectories of Change on the Earth's Surface. Kluwer Academic Publishers, Dordrecht,
699 pp 185-208

700 Wheeler CW, Archer SR, Asner GP, McMurtry CR (2007) Climate and edaphic controls on soil
701 carbon-nitrogen responses to woody plant encroachment in desert grassland. *Ecol Appl*
702 17:1911-1928

703 Wilcox BP, Pitlick J, Allen CD, Davenport DW (1996) Runoff and erosion from a rapidly eroding
704 pinyon-juniper hillslope. In: Anderson MG, Brooks SM (eds) *Advances in Hillslope*
705 *Processes*, vol Volume 1. John Wiley & Sons Ltd, New York, pp 61-77

706

707

708

709 **Figure Legends**

710

711 Figure 1. Soil organic C and total (inorganic and organic) soil C in three vegetation microsites at
712 the Jornada Basin LTER. Error bars are standard error for microsite replicates ($n = 10$
713 replicates microsite⁻¹). Within each of the two C groupings (organic C and organic + inorganic
714 C), different letters indicate a significant difference among vegetation microsites.

715

716 Figure 2. Soil carbon in light, heavy, soluble, and carbonate fractions in the three vegetation
717 microsites at the Jornada Basin LTER. Results are from the two density fractionation. Error
718 bars are standard error for microsite replicates ($n = 10$ replicates microsite⁻¹). Within a fraction,
719 different letters indicate a significant difference among vegetation microsites.

720

721 Figure 3. Patterns of a) soil organic N and b) soil C:N in the three vegetation microsites at the
722 Jornada Basin LTER. Results are from the two density fractionation. Error bars are standard
723 error for microsite replicates ($n = 10$ replicates microsite⁻¹). Within a fraction, different letters
724 indicate a significant difference among vegetation microsites.

725

726 Figure 4. Patterns of a) soil organic carbon and b) soil organic C:N for the seven density
727 fractionation from shrub subcanopy and grass microsites at the Jornada Basin LTER. Error
728 bars are standard error for analytical replicates of each sample ($n = 3$ replicates sample⁻¹).

729

730 Figure 5. $\delta^{13}\text{C}$ in light ($\leq 1.85 \text{ g cm}^{-3}$) and heavy ($> 1.85 \text{ g cm}^{-3}$) soil fractions in the three
731 vegetation microsites at the Jornada Basin LTER. Error bars are standard error for microsite
732 replicates ($n = 10$ replicates microsite⁻¹). Within a fraction, different letters indicate a significant
733 difference among vegetation microsites.

734

735 Figure 6. $\delta^{13}\text{C}$ for the seven density fractionation from shrub subcanopy and grass microsites
736 at the Jornada Basin LTER. Error bars are standard error for analytical replicates of each
737 sample ($n = 2$ replicates sample⁻¹).

738

739 Figure 7. Patterns of a) soil organic carbon and b) $\delta^{13}\text{C}$ in soil sequential density fractions from
740 shrub and grass microsites at the Jornada Basin LTER plotted in comparison with data from
741 soils studied by Sollins et al. (2009). Grassland and shrub sites are plotted with closed
742 symbols, forests with open symbols.

743

744 Figure 8. The proposed 5-pool model of dryland surface soil carbon. In this model, carbonate
745 dust, CO_2 from the atmosphere, and plant root and litter decomposition activity can influence the
746 formation of pedogenic carbonates. Light fraction ($\leq 1.85 \text{ g cm}^{-3}$) material can decompose into a
747 soluble but not mobilized pool in soil or can contribute to aggregate or mineral-associated C via
748 microbial activity and transport. Aggregate and organo-mineral complexes together comprise
749 the heavy fraction ($> 1.85 \text{ g cm}^{-3}$) pool. With woody encroachment (WE), the soluble pool and,
750 at least initially, the light fraction pools increase. Surface carbonate C may increase with WE
751 due to surface soil erosion, exposing lower horizon carbonates.

Fig. 1

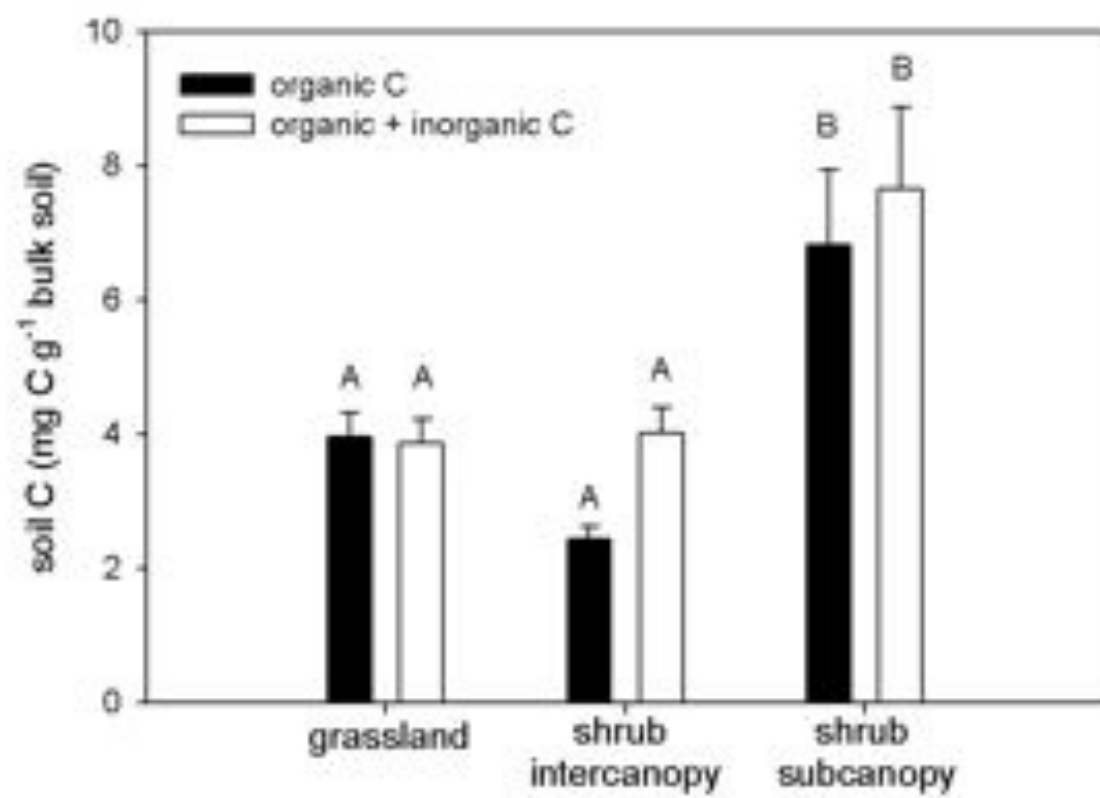


Fig 2

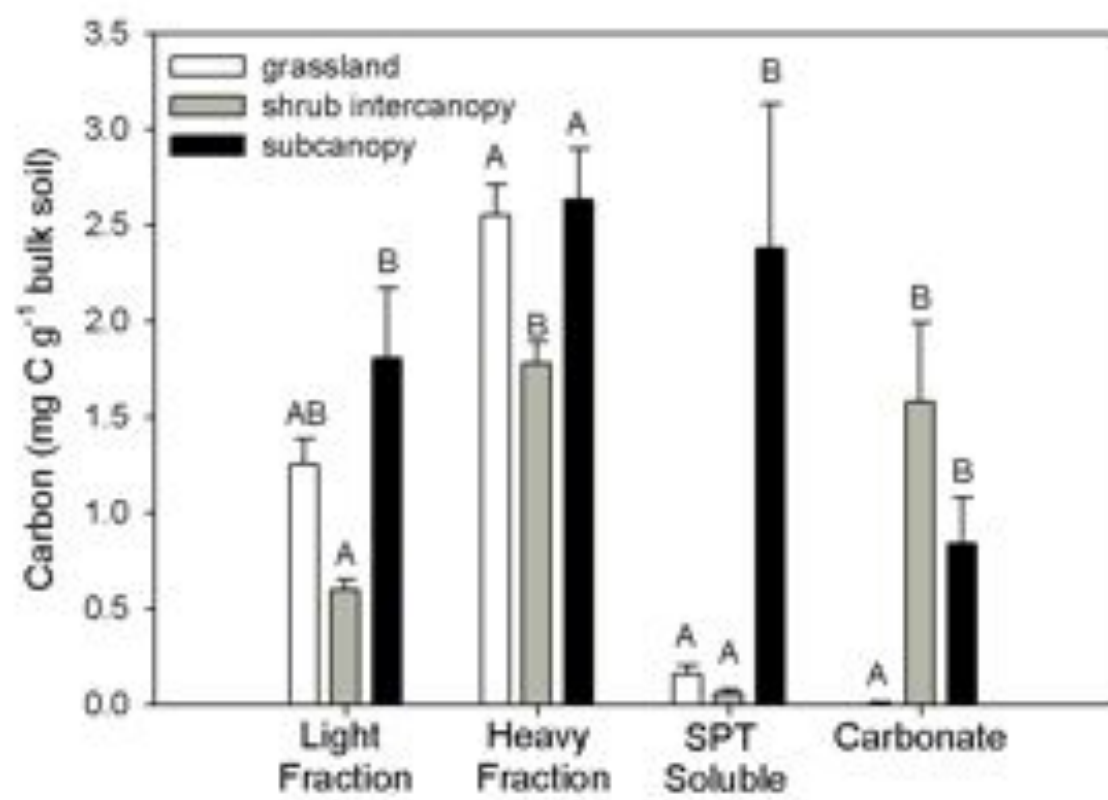


Fig. 3

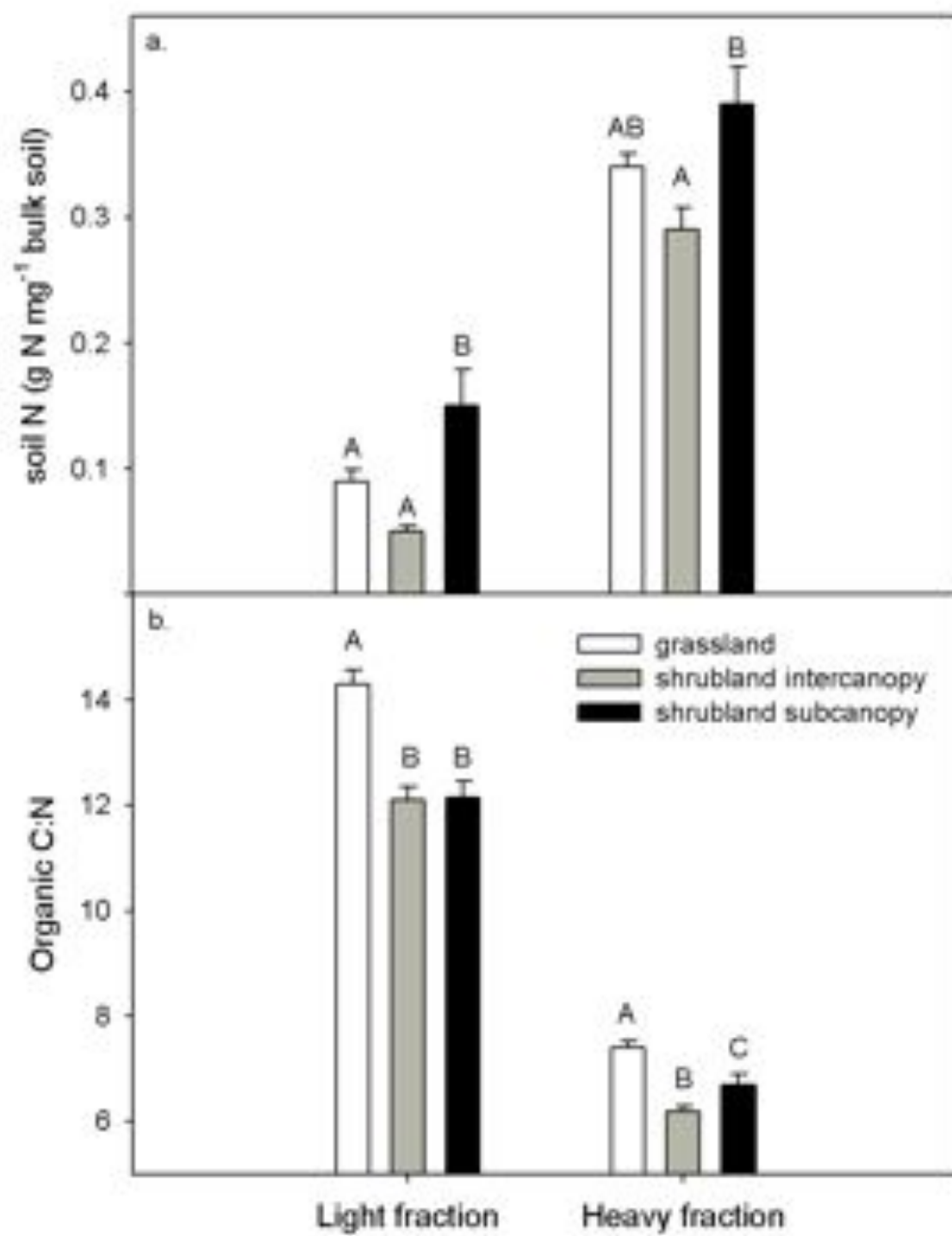


Fig. 4

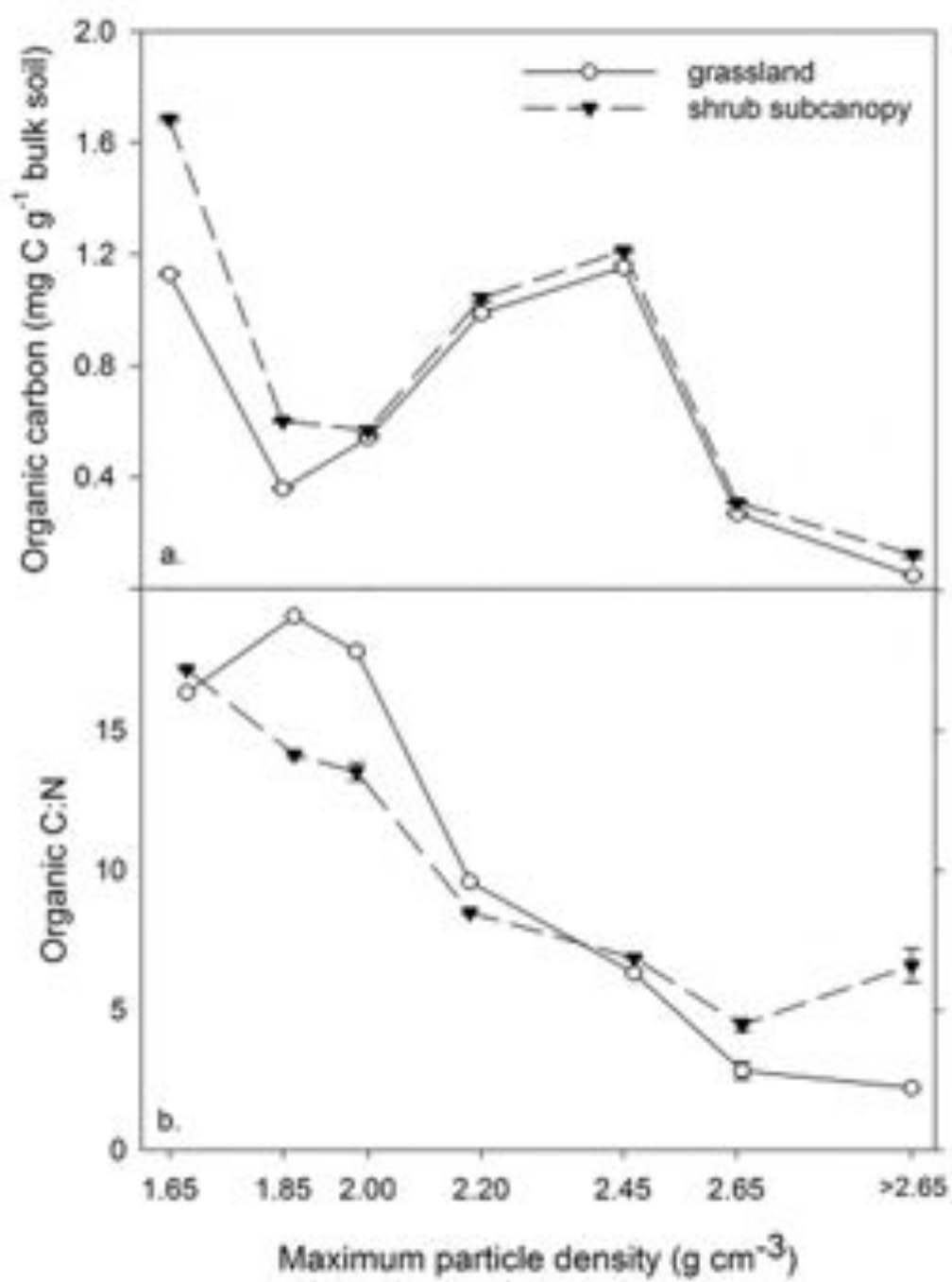


Fig. 5

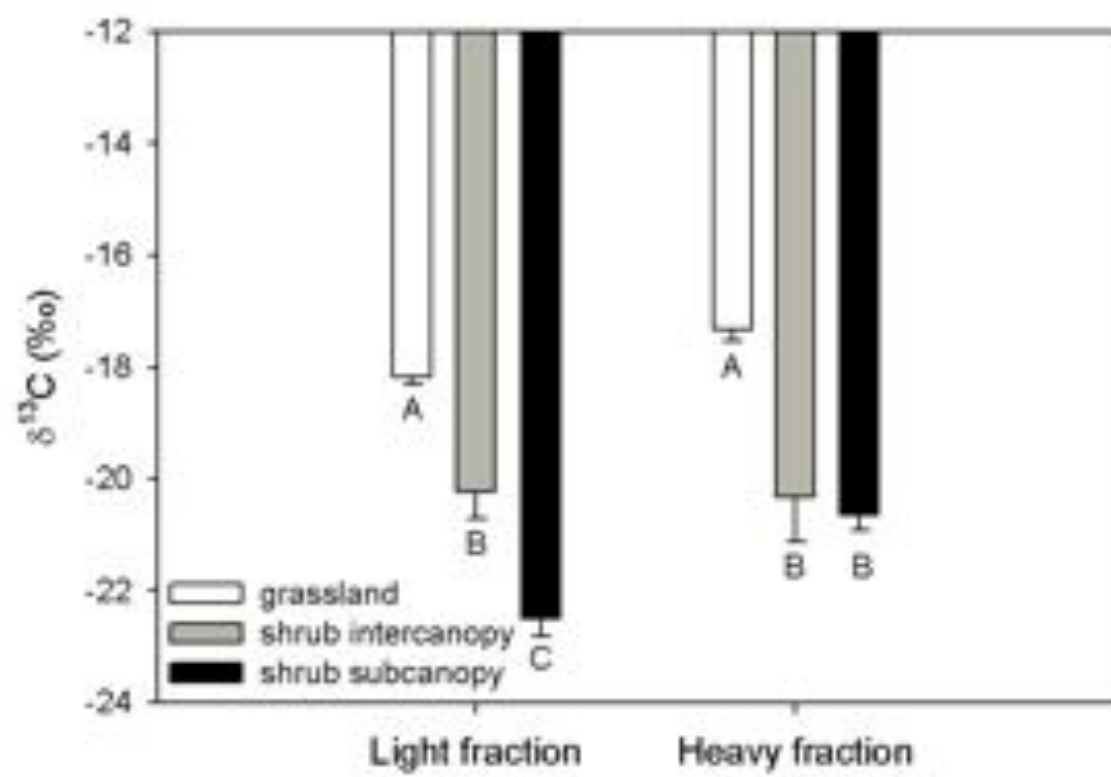


Fig. 6

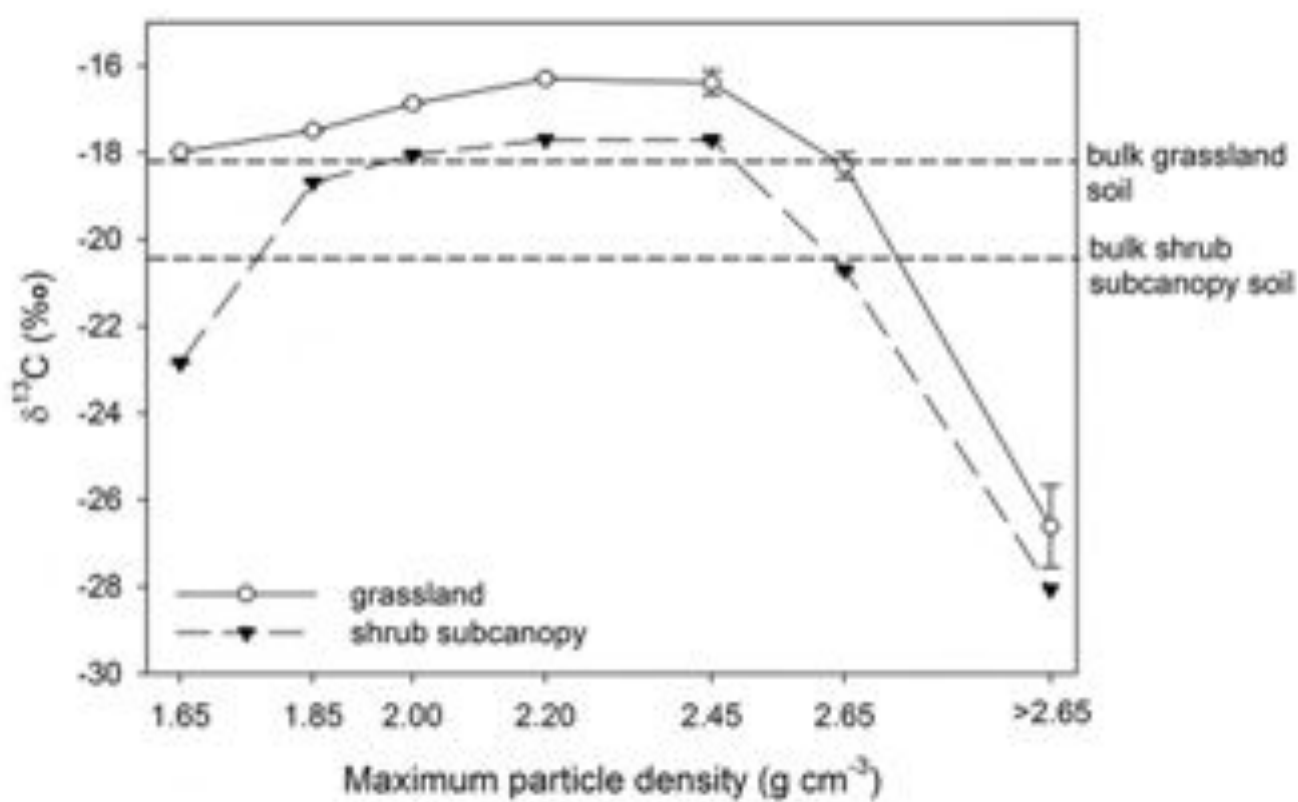


Fig. 7

